AAS 11-632

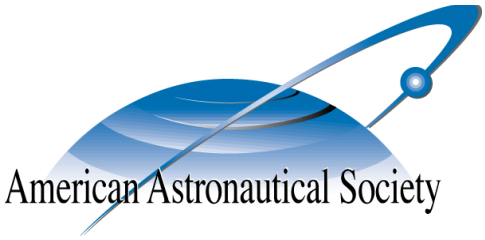

American Institute of
Aeronautics and Astronautics

ANALYSIS OF A TETHERED COULOMB STRUCTURE APPLIED TO CLOSE PROXIMITY SITUATIONAL AWARENESS

Carl R. Seubert, Stephen Panosian, and Hanspeter Schaub

University of Colorado, Boulder, CO 80309

AAS/AIAA Astrodynamics Specialists Conference

Girdwood, Alaska July 31 – August 4, 2011

AAS Publications Office, P.O. Box 28130, San Diego, CA 92198

(Preprint) AAS 11-632

ANALYSIS OF A TETHERED COULOMB STRUCTURE APPLIED TO CLOSE PROXIMITY SITUATIONAL AWARENESS

Carl R. Seubert,* Stephen Panosian,† and Hanspeter Schaub‡
University of Colorado, Boulder, CO 80309

A unique tether application for situational awareness at geosynchronous altitudes is investigated. The relative dynamics between a small sensor platform tethered to a large host-spacecraft is examined. Charging both craft to $|30|$ kV holds the relative dynamics fixed in the presence of gravitational and solar radiation forces. Numerical simulations illustrate the use of multiple tether connections increases the stiffness and allows 10 m separated craft to yield relative shape variations less than 50 mm in translation and 5 degrees in attitude. It is also shown that in nominal plasma conditions less than 20 W of power along with only grams of propellant are required to maintain spacecraft potentials.

INTRODUCTION

The time and monetary investments it takes to launch a satellite to a Geosynchronous orbit (GEO) prompts many precautions to be taken in satellite designs and operation. Because of the large risks involved in developing and launching a successful large GEO spacecraft, as well as the issues of determining if these large space structures have deployed properly, there is a need for a local close proximity situational awareness. This sensing can incorporate visual confirmation of mechanism deployment and operations as well as spacecraft and local environment information collection.

Local inspection can be an invaluable feature when diagnosing spacecraft performance or monitoring the surroundings for spacecraft and/or debris. However, actually conducting close proximity situational awareness is problematic. Japan's IKAROS mission ejected a free-flying camera in order to get final images and confirmation of its solar sail deployment.[1] This method however, provides only single use and is not practical for GEO because it only adds to the growing space debris problem. Closed relative orbits can be used for situational awareness to keep a secondary spacecraft within a certain proximity of a primary spacecraft.[2] However, this results in the need for a complete secondary spacecraft with all major subsystems, thus increasing mission costs and mass and the risks for system failures. Additionally, this does not provide a constant relative reference point and requires significant sensing, control and propellant. These current technologies show that there is a discontinuity between what technology is available and what is needed for spacecraft close proximity operations.

Several, essentially propellantless, concepts in recent years that address the needs of free-flying proximity operations are the use of Coulomb,[3,4] magnetic and flux-pinning,[5,6] or Lorentz forces.[7] Of specific interest is the use of inter-spacecraft Coulomb forces to conduct close formation relative

*Graduate Research Assistant, Aerospace Engineering Sciences Department, AAS & AIAA student member
†Graduate Research Assistant, Aerospace Engineering Sciences Department, AAS & AIAA student member
‡Associate Professor, H. Joseph Smead Fellow, Aerospace Engineering Sciences Department, AIAA Associate Fellow, AAS member

control because of its low power and propellant requirements.[3,4,8] This work examines a new concept, the Tethered Coulomb Structure (TCS), and its use for close proximity situational awareness at GEO.

The TCS concept provides a means of creating semi-rigid structures in space using Coulomb forces and spacecraft interconnected with fine, low mass tethers.[9,10] Using continuous charge emission the spacecraft nodes are charged to kilovolt potentials and repelled, holding the tethers in tension. A benefit of the TCS system is that the interconnecting tethers restrict relative translational and rotational motions, providing a continuous close proximity platform that can be used for situational awareness. A key advantage of a TCS is that it would have long-term mission capability because, it only requires Watt-levels of power and low propellant mass.[9] A benefit of a TCS system over free-flying Coulomb formation is that a TCS does not require precise charge levels to maintain relative positions due to its shape being constrained by the tethers. Spacecraft charge levels must only be maintained above a certain threshold for which the TCS system would be robust to orbital perturbations such as differential gravity and solar radiation pressure. Additionally, relative attitude control between spacecraft nodes will be negligible when the Coulomb and tensile forces are in equilibrium.

Using a TCS system does however have its limitations. Space plasma reduces the Coulomb force between spacecraft nodes making it challenging to implement in low Earth orbit. The plasma is characterized by the Debye length (λ_D) which at GEO is large providing minimal force shielding. Three representative GEO plasma conditions (quiet, nominal, and disturbed), previously defined in Reference 11, define the extreme bounds and nominal operating regimes a TCS spacecraft will encounter on orbit. The Debye lengths corresponding to these plasmas is: Quiet: $\lambda_D = 4$ m, Nominal: $\lambda_D = 200$ m, and Disturbed: $\lambda_D = 743$ m. The quiet plasma ($\lambda_D = 4$ m) bounds the 'worst-case' conditions at GEO and are only characteristic of extreme times. Nominal plasma conditions are a closer representation of the typical operating conditions at GEO, while a disturbed environment is the lower limit of power requirements and force shielding.

One envisioned use of a TCS is to provide local situational awareness for a geosynchronous satellite. Here one large spacecraft (the Mother) has a smaller spacecraft (the Child) tethered to it as illustrated in Figure 1. Both craft are spherical and feature an outer conducting surface for charge distribution. This Mother-Child (MC) application of a TCS can provide a unique vantage point for on-orbit inspection of the Mother craft, rendezvous, docking and refueling operations and space environment measurements. The key advantage that a TCS can provide for situational awareness at GEO is that it can hold a Child spacecraft at a relatively fixed position and attitude with respect to the Mother craft with minimal sensing, control and propulsion needs. It is expected that the Child craft is a small, low mass craft with only minimal or essential hardware.

The intent of this paper is to explore this specific application of the TCS concept. This involves quantifying the plausible MC operating configurations and the resulting dynamics and power requirements. Previous research on the TCS concept investigates relative motion without nodal rotation[9] as well as simplified two-dimensional translational and rotational motion about one axis.[10] A full three-dimensional study is conducted for two identical TCS nodes,[11] but does not simulate naturally unstable on-orbit configurations or large mass ratios. This study expands upon previous research by simulating two non-identical (size or mass) TCS nodes (Mother and Child) in naturally unstable orbit configurations.

The objectives of this work and an outline of this paper is as follows. Of interest is the extent of

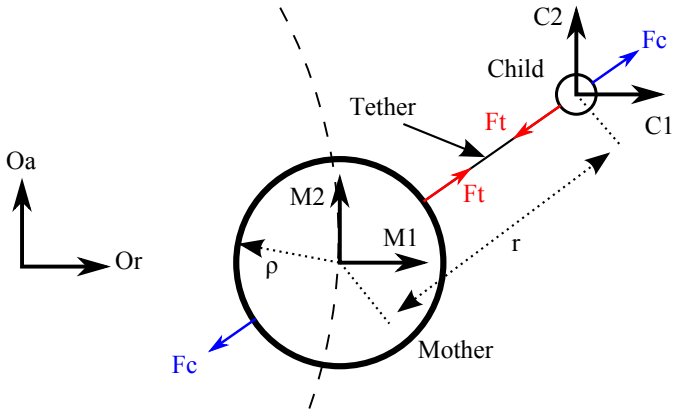

Figure 1. Illustration of tethered Mother Child spacecraft application

relative rotation and translation between the mother and child vehicles. The influential forces and equations of motion for a TCS are presented along with the parameters of the Mother-Child baseline application. Numerical simulation results are presented to show plausible MC operating regimes and resulting dynamics. The effects of spacecraft potential on required power and dynamics is studied. The technological means of charging the spacecraft and resulting propellant mass needs for continuous MC operations are given. Lastly, the mass of the Child craft is investigated to quantify its effects on the MC relative dynamics.

EQUATIONS OF MOTION

This section develops the Coulomb force between the charged Mother and Child craft in a plasma and presents the resulting translational and rotational equations of motion for this TCS application.

Electrostatic Force Modeling

A Coulomb force is generated from the electrostatic interaction of two charged bodies. Consider the isolated Mother that is a finite sphere of radius ρ_M, with a surface potential V_M in a plasma will have a potential field represented by the Debye-Hückel equation:[12,13]

$$V(x) = \frac{V_M \rho_M}{x} e^{-(x-\rho_M)/\lambda_D} \tag{1}$$

Here x is the center-to-center separation distance. This equation is only valid if a small spacecraft potential compared to the local plasma thermal energy is assumed ($e_c V \ll \kappa T_e$), where $e_c = 1.602176 \times 10^{-19}$ C is the elementary charge, $\kappa = 1.38065 \times 10^{-23}$ JK^{-1} is the Boltzmann constant and T_e is the plasma electron temperature in Kelvin. In a nominal GEO plasma the ($e_c V \ll \kappa T_e$) condition is no longer true if the spacecraft charges to >1-10 kV potentials. The Debye-Hückel equation is derived from neglecting the higher order terms of Poisson's partial differential equation which results in less plasma shielding of the electrostatic fields, and represents a conservative estimate.[14] The benefit of using Equation (1) is that it allows for simplified analysis, and faster numerical simulations because the full Poisson-Vlasov equations do not need to be solved. Solving the full Poisson-Vlasov equations requires solving complex partial differential field equations.

Equation (1) is differentiated to obtain the electric field (E-field) of the isolated sphere and rearranged to obtain the relationship between charge and potential in a plasma:

$$V_M = \frac{q_M k_c}{\rho_M}\left(\frac{\lambda_D}{\rho_M + \lambda_D}\right) \tag{2}$$

If this plasma has minimal interaction ($\rho_M \ll \lambda_D$) this charge on the isolated sphere reduces to the classical vacuum formulation ($V = qk_c/\rho$) as required. If a second charge q_C (Child) is placed at a distance r in the E-field of the mother the resulting Coulomb force, which is also a conservative estimate[14] is computed using:[11]

$$|\boldsymbol{F}_c| = k_c \frac{q_M q_C}{r^2} e^{(-(r-\rho_M))/\lambda_D}\left(1 + \frac{r}{\lambda_D}\right) \tag{3}$$

where $k_c = 8.99 \times 10^9\ \mathrm{Nm^2C^{-2}}$ is the vacuum Coulomb constant. To account for the influence of charged finite spheres in close proximity in this Coulomb force equation it is necessary to compute the combined capacitance of the system. This is achieved by using Eq. (2) which gives the potential of the Mother and including the potential of the Child craft,[15,16] at a distance r, using the equivalent form of Eq. (2) substituted into the Child equivalent of Eq. (1) giving the relationship of the MC system:

$$V_M = \frac{q_M k_c}{\rho_M}\left(\frac{\lambda_D}{\rho_M + \lambda_D}\right) + \frac{k_c q_C}{r}\left(\frac{\lambda_D}{\rho_C + \lambda_D}\right) e^{-(r-\rho_C)/\lambda_D} \tag{4}$$

where ρ_C is the radius of the Child. Similarly, there is an equivalent potential equation for the Child and combined we obtain a system of linear equations:

$$\begin{bmatrix} V_M \\ V_C \end{bmatrix} = k_c \begin{bmatrix} \frac{1}{\rho_M}\left(\frac{\lambda_D}{\rho_M+\lambda_d}\right) & \frac{1}{r}e^{\frac{-(r-\rho_C)}{\lambda_D}}\left(\frac{\lambda_D}{\rho_C+\lambda_D}\right) \\ \frac{1}{r}e^{\frac{-(r-\rho_M)}{\lambda_D}}\left(\frac{\lambda_D}{\rho_M+\lambda_D}\right) & \frac{1}{\rho_C}\left(\frac{\lambda_D}{\rho_C+\lambda_D}\right) \end{bmatrix} \begin{bmatrix} q_M \\ q_C \end{bmatrix} \tag{5}$$

This combined capacitance has a significant influence on the effective charge of each sphere, with fixed potentials, when the center-to-center separation is low relative to the sphere radii (separations less than approximately 10 sphere radii, ($r < 10\rho$).

The simulations for this study specify a constant and equivalent potential $V_M = V_C$ for the spacecraft, which is a nominal TCS application characteristic. Using this desired potential, Eq. (5) is inverted to solve for the resulting charges which are used to compute the repulsive Coulomb force using Eq. (3). Uneven charge distribution on the conducting spacecraft surfaces is not considered in this analysis for simplicity and is only really significant for very close separations ($r < 3\rho$).

TCS Forces

The numerical simulation of this study computes the translational and rotational motion of TCS nodes. The only forces assumed to be acting on a TCS at GEO are Coulomb, tensile, gravity, and solar radiation pressure. The Coulomb force of Eq. (3) given in the previous section is included with the remaining forces discussed here.

The tethers are modeled as a proportional spring with nonlinear end displacements. This allows for general tether stretching due to arbitrary node translation and/or rotation. The magnitude of the

tensile force from a single tether is given by:

$$|\boldsymbol{F}_{\mathrm{s}}| = \begin{cases} k_{\mathrm{s}}\delta L & \delta L > 0, \\ 0 & \delta L \leq 0. \end{cases} \tag{6}$$

where k_s is the proportional spring constant and δL is the stretch in the tether. The spring constant is computed from the tether properties using the relationship ($k_s = EA/L$) where E, A and L are Young's modulus, tether cross-sectional area and the nominal tether length, respectively. For this work E and A are assumed to be 271×10^9 Pa and 5.29×10^{-10} m^2, respectively. These parameters are representative of the fine, low mass tether materials currently being considered for a TCS.

If the MC system features only a single connecting tether, Eq. (6) gives the total tether force on each node. However, the algorithm is capable of simulating multiple tethers between each node. The tether length increase of tether k between nodes i and j is defined by δL_{ijk}. Therefore, the resulting tensile force acting on node i from the tether(s) connected to node j is:

$$\boldsymbol{T}_{ij} = k_{\mathrm{s}} \sum_{k=1}^{M} \delta L_{ijk} \hat{\tau}_{ijk} \tag{7}$$

where M is the number of tethers between nodes i and j and $\boldsymbol{\tau}_{ij}$ is the vector defining the k^{th} tether's connections between node i to j.

A two-body gravity model is simulated for the TCS operating at GEO with a force:

$$|\boldsymbol{F}_g| = \frac{\mu m_i}{|\boldsymbol{R}_i|^2} \hat{R}_i \tag{8}$$

where $\mu = 3.986 \times 10^{14}$ m^{3}s^{-2} is the gravitational coefficient for Earth, m_i is the spacecraft node mass and $\boldsymbol{R}_i$ is the inertial position of node i.

The Solar Radiation Pressure (SRP) force at 1 AU is simulated using:

$$\boldsymbol{F}_{SRPi} = P_{SRP} C_r A_s \hat{S}_i \tag{9}$$

where P_{SRP}, C_r, and A_s are the solar radiation pressure, surface reflectivity and the cross-sectional area of the spacecraft, respectively and $\hat{S}_i$ is the unit vector from the Sun to node i.

Translational EOM

All four forces simulated at GEO (Coulomb, tensile, gravity and SRP) impact the translational equations of motion of a TCS node that is calculated by:

$$\ddot{\boldsymbol{R}}_i = -\frac{\mu}{|\boldsymbol{R}_i|^2}\hat{R}_i + P_{SRP} C_r A_s \hat{S}_i + \frac{\boldsymbol{T}_{ij}}{m_i} + \frac{k_c q_i q_j (-\hat{r}_{ij})}{m_i r_{ij}^2} e^{(-(r_{12}-\rho))/\lambda_D} \left(1 + \frac{r_{ij}}{\lambda_D}\right), \; i \neq j \tag{10}$$

Rotational EOM

It is assumed that the only torque driving the rotational motion of a TCS node is from the tether forces. Differential gravity and Solar radiation pressure induced torques can be ignored because the spacecraft are spherical and have symmetric mass moments of inertia. With even charge distribution

on the conducting spheres the Coulomb forces act on the center of each node producing no torque. Therefore, the attitude of each spacecraft node is dependent on the torque from each tether:

$$^{\mathcal{B}}\mathbf{\Gamma}_i = \sum_{k=1}^{M} \left(^{\mathcal{B}}\boldsymbol{p}_{ijk} \times [\mathcal{BI}]_i {}^{\mathcal{I}}\boldsymbol{T}_{ijk} \right) \quad , \quad i \neq j \tag{11}$$

where $\boldsymbol{p}_{ijk}$ is the body fixed vector that defines the location of the k^{th} tether attachment point on node i that connects to node j and $[\mathcal{BI}]_i$ is the direction cosine matrix of the attitude of node i relative to the inertial frame. The angular acceleration of each node is defined in the body frame with Euler's rotational equations of motion:[2]

$$[I]_i \dot{\boldsymbol{\omega}}_i = -\boldsymbol{\omega}_i \times ([I]_i \boldsymbol{\omega}_i) + \mathbf{\Gamma}_i \tag{12}$$

The attitude of each node is represented with the modified rodrigues parameters (MRP) which are integrated using the differential kinematic equation:

$$\dot{\boldsymbol{\sigma}}_i = \frac{1}{4} \left[(1 - \sigma_i^2)[I_{3\times 3}]_i + 2[\tilde{\boldsymbol{\sigma}}]_i + 2\boldsymbol{\sigma}_i \boldsymbol{\sigma}_i^T \right] \boldsymbol{\omega}_i \tag{13}$$

The MRP set will go singular with a rotation of $\pm 360^\circ$. To ensure a non-singular description, the MRP description is switched to the shadow set whenever $|\boldsymbol{\sigma}| > 1$.[2]

MOTHER-CHILD CONFIGURATION

This section outlines the parameters of a baseline two node, Mother Child configuration used for simulations and presents both natural and controlled dynamics of this TCS application. The trivial set up for this MC configuration is to have the two craft in a orbit radial alignment. Under differential gravity, this set up would maintain a taut tether and constant shape without charge, but would be less robust to perturbations. Charging the spacecraft allows for additional configurations with negligible relative translation and rotation motions. This section uses numerical simulations to examine the requirements of a TCS to hold a Child craft fixed relative to the Mother in an arbitrary orbit configuration. Unless otherwise stated, the Mother and Child are modeled as spheres with masses and radii of 2000kg, 2m, 50kg and 0.5m, respectively. All other baseline simulation parameters are listed in Table 1. Additionally, the spacecraft system begin each simulation with an inertial rotation rate equal to that of the orbit frame (360 deg/day).

Table 1. Mother Child baseline simulation parameters

Nodal surface potential	30 (kV)
Center to center separation	7 (m)
Mass moment of inertia	Solid Sphere
Tether spring constant	35.8398 (Nm^{-1})
Debye length λ_d	200 (m)
SRP at 1 AU P_{srp}	4.56e-6 (Nm^{-2})
Surface reflectivity C_r	1
Simulation duration	24 hrs

Tethered Structure vs TCS

A configuration of more interest than an orbit radial alignment, is when the Child is placed at an arbitrary position relative to the Mother craft. One such example would be placing the Child craft where it would have positive radial and along track components relative to the Mother craft. Figure 2 graphically shows time elapsed snapshots of a tethered structure (TS) and TCS for this baseline two node system with system parameters given in Table 1. From Figure 2 it can be seen that for a TS (left) the relative position and attitude of the two craft varies over an orbit from an initial stationary relative separation and attitude. The tether is mostly slack and after only 5 hours there is a significant relative rotation between the Child and Mother. The TCS (right) however, maintains a reasonably fixed relative position and rotation between the two craft. Figure 3 shows numerically the small relative position and rotation difference between the Mother and Child craft in this simulation. The relative attitude here and in all subsequent simulations is calculated as the Euler principal rotation about the principal axis. The reason for the small relative motion deviations is that the tether between the two craft remains almost always in tension throughout the orbit. The constant tension restricts the variations in relative distance and rotation to less than 4 mm and 1 degree, respectively. Thus, this shows a single-tether TCS can be used to hold a Child craft relatively fixed in relation to a Mother spacecraft. These results are also typical if the Child craft has an out of plane position, relative to the Mother craft.

Fixed Mother Craft

Figure 3 shows that the relative positions and rotations between a Mother and Child TCS can be kept nearly constant for arbitrary initial orbit alignment. However, the system as a whole does under go rotation relative to the orbit frame. This contradicts a common GEO attitude requirement to remain fixed relative to the orbit frame. This can be addressed by implementing a simple and stable attitude control solution to fix the mothers pointing in the orbit frame using:

$$\boldsymbol{u} = -[A]\boldsymbol{\sigma} - [B]\boldsymbol{\omega} \tag{14}$$

where $[A]$ and $[B]$ are positive definite gain matrices.[2] Including this control in the Mother's rotational equations of motion of Eq. (12) gives:

$$[I]_M\dot{\boldsymbol{\omega}}_M = -\boldsymbol{\omega}_M \times ([I]_M\boldsymbol{\omega}_M) + \boldsymbol{\Gamma}_M + \boldsymbol{u} \tag{15}$$

This control torque, $\boldsymbol{u}$, is assumed to be applied by an internal momentum wheel system on the Mother craft. Figure 4 shows the relative numerical results for a MC configuration implementing the control of Equation (14). In this scenario the Mother craft orientation is held fixed, while the tethered Child spacecraft is free to translate and rotate due to the differential gravity, SRP, Coulomb and tether forces. Of interest is the magnitude of the relative Child motions in this scenario. The parameters for this simulation are given in Table 1 and the control is implemented at 1 Hz with gains of 100. These gains are chosen based on predicted performance to hold the Mother craft fixed in the orbit frame. This control torque is implemented in all future simulations.

From Figure 4(a) it can be seen that the Child craft position attempts to move in the positive radial and negative along track directions, which is expected for a craft with an initially larger orbit. However, this motion is restricted by the tether and causes oscillations less than 50 mm in each direction. The top plot in Figure 4(b) shows the relative rotation between the Child and Mother craft, while the bottom plot illustrates the rotation of the Mother craft relative to the orbit frame.

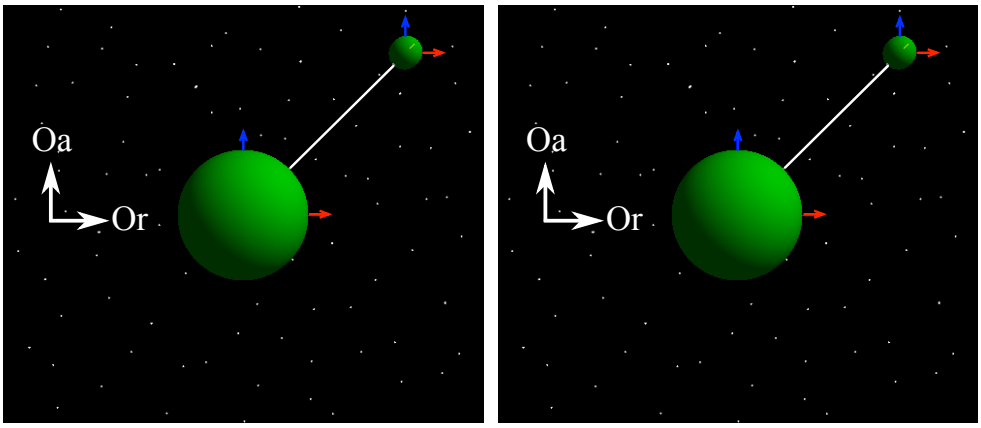

(a) TS at t = 0 hrs (b) TCS at t = 0 hrs

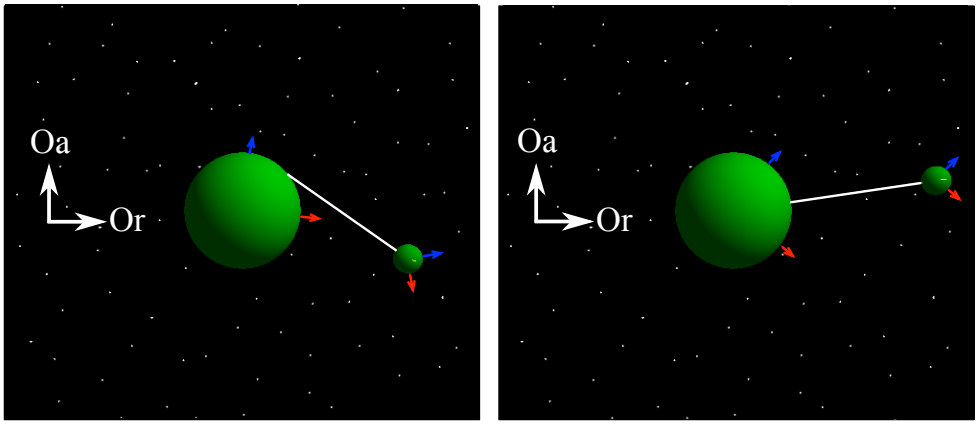

(c) TS at t = 5.5 hrs (d) TCS at t = 5.5 hrs

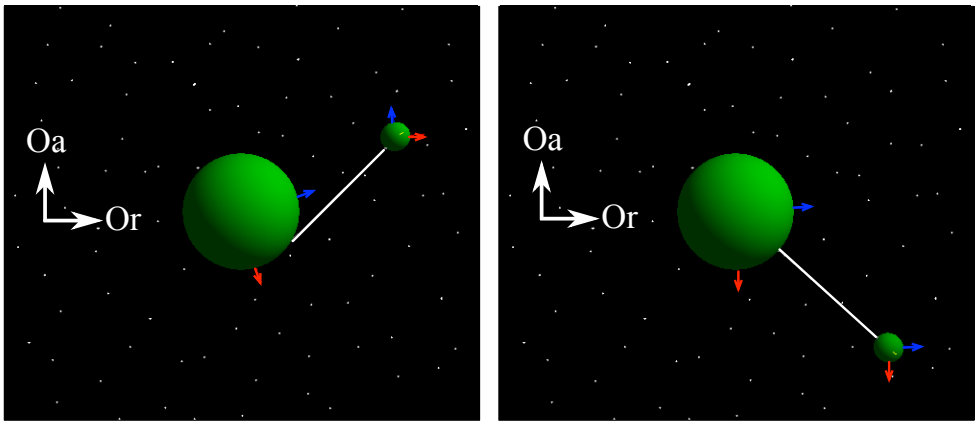

(e) TS at t = 14 hrs (f) TCS at t = 14 hrs

Figure 2. TS and TCS comparison of Mother Child configuration

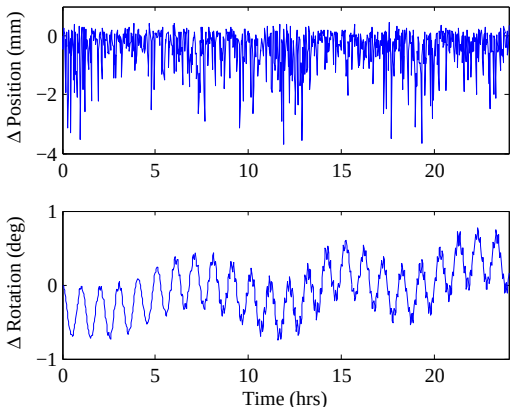

Figure 3. TCS Mother Child relative position and rotation

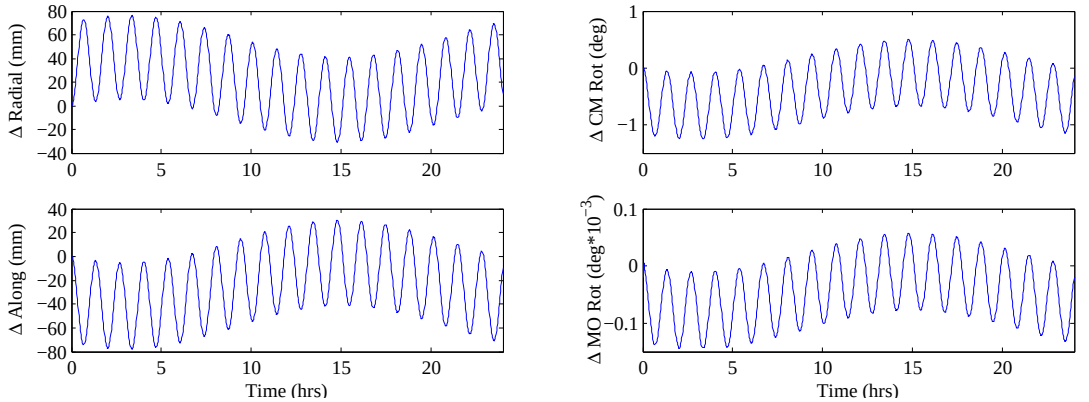

(a) Relative change in position

(b) Child/Mother & Mother/orbit relative attitudes

Figure 4. TCS Mother Child relative position and rotation with Mother attitude control

From the figure it can be seen that this simple control holds the Mother aligned with the orbit frame and subsequently the Child orientation is held within 1 degree of the Mother. As expected, the relative translational motion is larger than with the uncontrolled Mother attitude scenario, however still small with this Coulomb force. Additionally, simulations show that relative out of plane motion can also be constrained with this attitude control law. Since this TCS and control setup constrains the relative motion of the Child craft it is now beneficial to examine the affect of deviations in separation distances from this baseline MC configuration on the relative motion.

Relative Dynamics Due to Separation Distance Variations

The distance between the Mother and Child craft determines what operations the Child can perform, as well as what field of view the Child has of the Mother. The larger the separation distance between the two, the greater field of view the Child has of the Mother and surroundings for inspections and situational awareness. Of interest in this study is the affect of separation distance on the relative motions of the MC nodes. To obtain the most complex relative dynamics the Child craft is initially placed equally in the radial, along and cross track directions.

In addition to varying the separation distances, additional tethers between the spacecraft nodes are implemented to examine enhanced relative motion constraints as initially described in Reference 11. Figure 5 shows the maximum relative rotation between the Mother and Child, maximum variation in separation distance and required control torques for various MC separation distances. These results serve as a measure of the stiffness of a MC TCS. All three plots in Figure 5 show that increasing separation distance increases the maximum relative rotation, the maximum separation from equilibrium and the required torque. The required torque is the total net sum for an entire 24 hour orbit and Figure 5(c) shows that the amount required is well within what is feasible with current momentum wheel systems on a GEO spacecraft.

Figures 5(a) & 5(b) show that increasing the tether number reduces rotations and variations in separation distance of the MC TCS. Using a triple tether configuration can reduce the maximum relative rotation by up to 60%. Figure 5(a) demonstrates that separation distances upwards of 10 m can still provide reasonable relative rotations of about five degrees for this scenario with the Child in the radial, along and cross track directions. Additionally, the results of Figure 5(b) show that there will only be centimeter level variations in separation distance between the two craft.

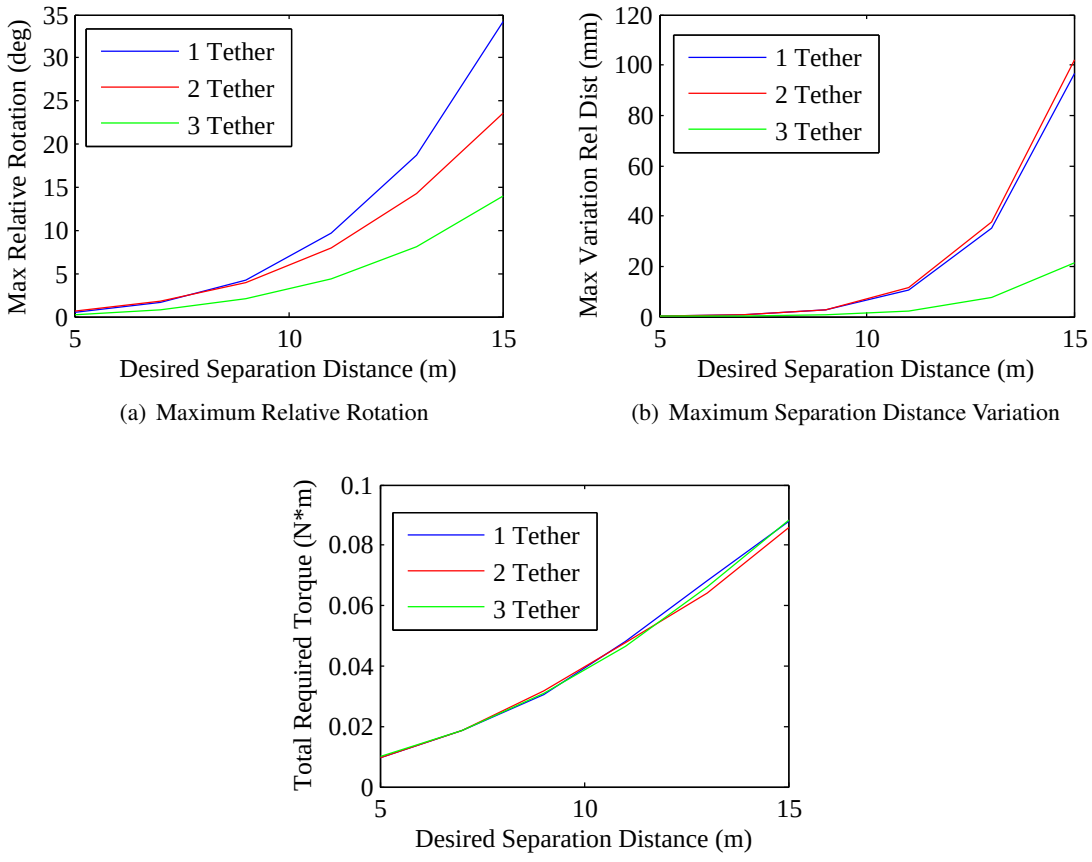

(a) Maximum Relative Rotation

(b) Maximum Separation Distance Variation

(c) Required Attitude Control Torque

Figure 5. Mother Child relative dynamics as a function of separation distance

MC POWER REQUIREMENTS AND POTENTIAL CONSIDERATIONS

The previous section shows that constrained relative motion between a Mother and Child can be achieved for an arbitrary orientation. However, in addition to the implemented control torque, it is also required that the spacecraft maintain elevated potentials for all time. This section analyzes the necessary power required to maintain the TCS at desired potentials in GEO space plasma conditions. Additionally, the effects of the spacecraft polarity on the required power is examined for various potentials. Lastly, the effects of varying the spacecraft potential on the relative dynamics of the MC TCS is investigated.

Coulomb Power Requirements

The net power required for a charged spacecraft to maintain a fixed potential in a plasma is directly proportional to the spacecraft potential and the net current from the plasma. This is represented with $P = V_{sc} I_{\text{net}}$, where V_{sc} is the spacecraft potential relative to the plasma and I_{net} is the net plasma current. It is assumed the plasma is comprised of two populations (electrons, protons) that are modeled with single-Maxwellian distributions. A spacecraft at GEO is stationary relative to the plasma (no ram currents) and the two primary current contributions are from electron and ion bombardment. The net plasma current is developed for both positive and negatively charged spacecraft in Reference 11 using the Boltzmann factor representation and exponential repulsion and Mott-Smith and Langmuir attraction.[17,18] The net plasma current also includes a third contribution, the photoelectron current on sun-lit surfaces. For this particular study only sun-lit conditions will be analyzed for power requirements as a spacecraft at GEO may be in eclipse for only minutes at a time in a 24 hour orbit. However, during these minimal eclipse periods is when the spacecraft can naturally and safely charge to kilovolt potentials. A charge feature that can be utilized by the TCS concept.

The combined power required to equally charge both the 2 m radius Mother and 0.5 m radius Child for each of the plasma conditions is shown in Figure 6. The range of spacecraft potentials used in this analysis is -30 to 30 kV, a reasonable range that is anticipated for TCS operations. The total power required of the MC system in a nominal plasma (λ_d = 200 m) is 8.2 W for -30 kV and 17.2 W for 30 kV. This is a realistic power consumption for a large GEO spacecraft. In the worst-case and rarely experienced quiet plasma (λ_d = 4 m) the power required by the system to maintain -30 kV is 181 W, and to achieve 30 kV requires 7439 W.

These power requirements are independent of the separation distances of the spacecraft. A consideration for the system is whether the Mother will feature a single charge control device that charges both itself as well as the Child through a conductive tether. An alternative is to have a charge control device on each craft that operates independently. Considering the eclipse operating environment, the craft have an equivalent power requirement during positive charging as this is independent of the photoelectron current. During negative charging, the net plasma current is lower and hence the power requirements are lower than this sun-lit case.

Potential Effects on Dynamics

In addition to its effects on power consumption, potential of the spacecraft will also affect the dynamics of the MC configuration.

The results of the previous section shows that lower potentials require less power, however a compromise is sought that also provides suitable constraints on the MC relative dynamics. Simulations

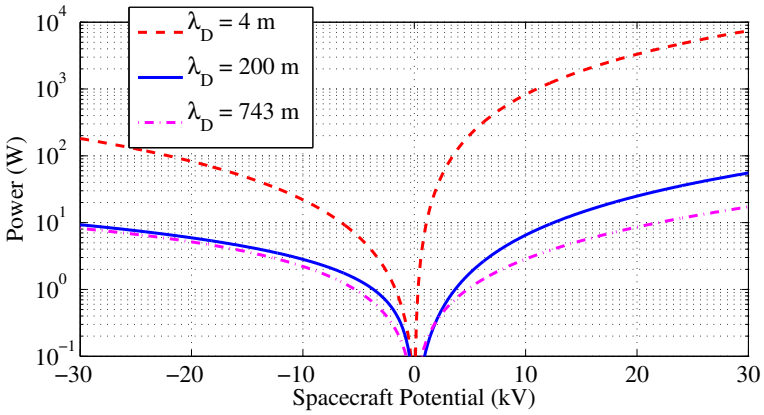

Figure 6. Power required in sun light to maintain fixed spacecraft potential for each plasma

are run to show the effects that various spacecraft potentials have on the MC dynamics. However, unlike the previous power consumption analysis, the polarity of the spacecraft does not affect the repulsion force between the two spacecraft, so polarity will not be considered. For these simulations there is an identical potential on each craft, but in practice different potentials on each craft could be used to simplify the design of either craft. Again, a worst-case orbit configuration with the Child in all three orbit directions is used. All other parameters are listed in Table 1.

Figure 7 shows the maximum relative rotations and maximum variation in separation distance as a function of MC potential. Similar to the distance variation, Figures 7(a) & 7(b) show that additional tethers decreases the maximum relative rotations and separation variations. Additionally, these figures show that increasing potentials also decreases these relative quantities. However, increasing the potential beyond 30 kV provides little improved performance, thus 30 kV can be considered a nominal maximum potential for this baseline TCS application. This magnitude of potential is also technically achievable. Potentials lower than 30 kV could be used to decrease power consumption but system stiffness decreases nonlinearly with potential. Lastly, simulation results indicate that spacecraft potential has negligible effect on the required attitude control torque. This is expected because torque is dependent on the transverse force and the moment arm. Even so, this shows that the rigidity of the connection between the Mother and Child has no effect on the required control torque.

Positive and Negative Charging Considerations

It is shown that the power requirements of a TCS system is dependent on the polarity and magnitude of the potential and that increasing the charge (Coulomb force) reduces relative motions. An additional consideration for both power consumption and Coulomb force is the size of the spacecraft nodes. Larger nodes will generate a greater Coulomb repulsive force (for a given potential level) while also requiring a larger power requirement due to a larger surface area interacting with the plasma. Analyzed here is the force generation and power requirements of the baseline MC system in comparison to a equal radii, two sphere system.

The Coulomb force generated between the two spherical TCS nodes of potential V_{sc} is computed using the force of Eq. (3) with shielding from the nominal plasma (λ_d = 200 m). The total power required is also computed in this nominal plasma in sunlight (photoelectrons included). Both the

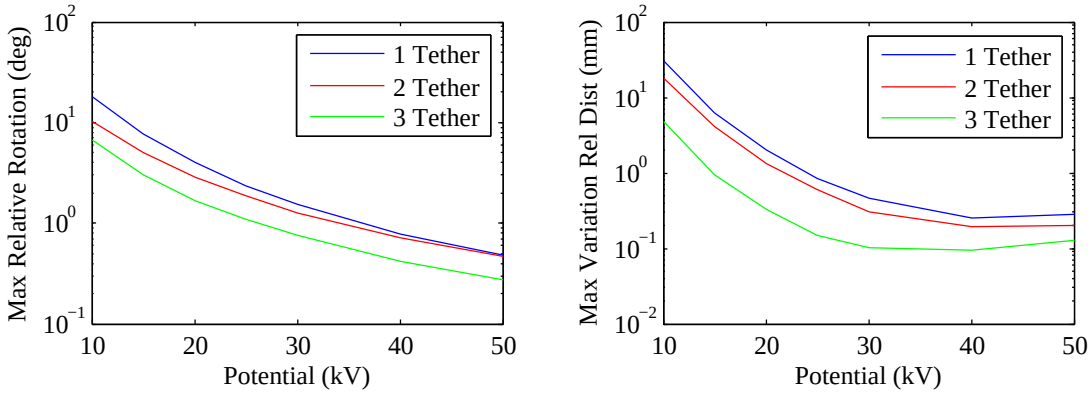

(a) Maximum Relative Rotation

(b) Maximum Separation Distance Variation

Figure 7. Mother Child relative dynamics as a function of craft potential

force and power is shown on a common axis as a function of spacecraft potential in Figure 8. The MC power and force is directly compared to a two node system of equal radii of three different values. In this figure the solid lines represent the required power, the dashed lines are the Coulomb force generated.

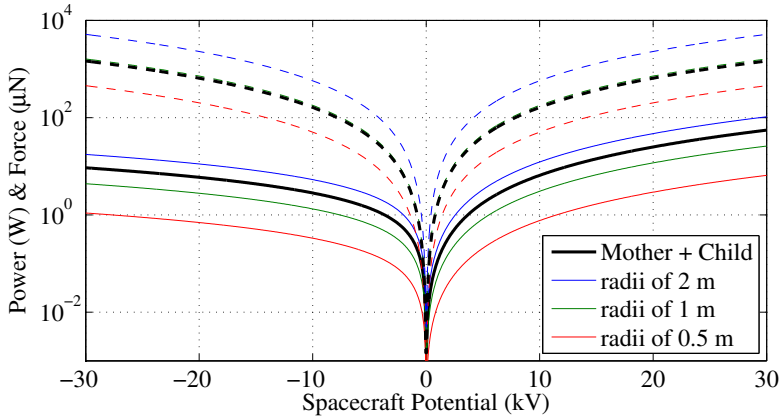

Figure 8 Force generated and total power required in sunlight [Solid = Power, Dashed = Force] as a function of sphere potential and radius. This is computed in a nominal plasma (λ_D = 200 m) with a center to center separation of 7 m.

Both the force and power are a function of $f(r^2)$, hence at a given potential the proportional increase between each radial line is equivalent. Ultimately, there is no optimal radii, TCS nodal size should be selected based on total power limitations, mass and size constraints or minimum force required for a given potential.

The Coulomb force is a function $F_c = f(V_{sc}^2)$ which dictates the shape of the curves, and is equivalent magnitude for both positive and negative potentials. The power required during positive charging is also a function $P(V_{sc} > 0) \approx f(V_{sc}^2)$ and hence has a similar profile to the force. However during negative charging in this nominal plasma, the dominant current is the constant photoelectrons and the resulting power is a function $P(V_{sc} < 0) \approx f(V_{sc})$. The result is that for negative charging lower power is required to achieve the equivalent force at a given potential.

To demonstrate the relationship between force and power, Figure 9 shows the ratio $\frac{F_c}{P}$ for the MC baseline setup. A large ratio value indicates more force is obtained per power required. This figure shows that for positive charging the ratio is constant. Figure 9 also shows that it is more advantageous to use negative charge, as an equivalent force can be generated for less power than the same positive charge.

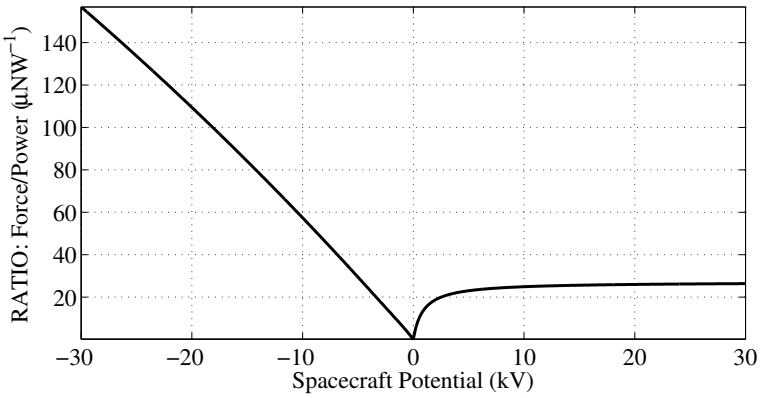

Figure 9 Ratio between force generated and power required in sunlight and a nominal plasma (λ_D = 200 m) for the baseline Mother Child system with a 7 m separation.

MC PROPELLANT MASS ESTIMATES

Another consideration for implementing a Coulomb repelled tethered Child on a GEO spacecraft is the amount of additional mass. Computed here is the mass required of the charge control device(s) and the associated propellant mass to maintain the desired surface potentials in the three representative plasma conditions (quiet, nominal, disturbed). Similar to the power analysis, the polarity of the spacecraft potentials will be a factor in the additional mass required and is addressed here. This is calculated for the baseline MC system with 2 m and 0.5 m radius spheres respectively, operating in sunlit conditions.

Charging Hardware

Charging of spacecraft in a space plasma is a natural process that can be regulated or enhanced for TCS purposes using a charge emission device. Previously, Figures 6 and 8 demonstrated that from a power perspective it is more advantageous to charge to negative potentials. Another consideration is the technology required for charge control. The technology for electron emission (positive charging) is less complex and electrons are freely available from solar energy. Alternatively, for negative charging, two primary charge control techniques that are effectively used in space are the hollow cathodes that emit noble gas ions and field emission using metal ions. It is envisioned that Coulomb formation and tethered structures will implement this space proven technology. An overview of a small set of these devices is given.

Hollow cathode emission typically accelerates gaseous ions of Argon, Krypton or Xenon that are typically stored in tanks up to 1000 psi.[19] SCATHA is a spacecraft that used both an electron gun and a Xenon ion beam for charging.[20] ProSEDS was intended for launch in 2003 with 245 g of Xenon for charge control. With a maximum emission current of 10 A at 200 μg/s, the system used 30 W, had a mass of 6 kg and dimensions of 20$\times$30$\times$13 cm.[21]

The alternate charge control device used in space is field evaporation with metal ions. The CLUSTER spacecraft emit Indium ions from a liquid source to maintain zero potential relative to the plasma. The emission current is 10-15 μA from an instrument that consumes less than 2.7 W and has a mass of 1.85 kg.[18,22] Similarly, the Geotail spacecraft uses two Indium ion emission devices of 1.8 kg, measuring 19×16×17 cm, with a current of 15 μA.

This gives an indication of the use of charge control devices in space but of importance here is the quantification of the mass, volume and power requirements of devices that could similarly be implemented on the MC TCS system.

Propellant Mass Flow Rates

For a TCS maintaining a fixed potential in a plasma, the required propellant and its mass flow rate is the charge control current emitted to offset the net plasma current. To charge to negative potentials positive ions from an on board propellant source are emitted. For this study the mass flow rate, during negative charging, is computed using Xenon gas ions (Xe^+). For charge control emission it is most advantageous to use the lowest mass particles (ideally H^+ ions), however Xenon is used as it is a common hollow cathode propellant and it results in the largest (worst-case) mass flow rate, with a higher ion mass than Indium (a common field emission propellant).[18,23] The mass flow rate, during negative charging, is computed using:[3]

$$\dot{m} = \frac{|I_{\text{net}}| m_{\text{ion}}}{e_c} \tag{16}$$

where m_{ion} is the mass of the emitted ion species assuming it has a single charge. For positive charging, m_{ion} is replaced with m_{electron}, the mass of an electron, which is 5 orders of magnitude less than Xenon gas ions. An advantage of using electrons is that they are essentially free propellant as they can be obtained on-orbit from solar energy. The instantaneous mass flow rate is directly proportional to the net plasma current and consequently power requirements and is computed for each plasma in a similar manner to Figure 6. Table 2 lists the combined MC maximum mass flow rates for each of the plasma conditions. The maximum rates correspond to the extremes of the analyzed spacecraft potentials of ±30 kV.

Table 2. Combined maximum mass flow rate [μgs^{-1}] for each plasma at a given spacecraft potential

Spacecraft potential	Quiet (λ_D = 4 m)	Nominal (λ_D = 200 m)	Disturbed (λ_D = 743 m)
-30 kV	8.24	0.42	0.37
+30 kV	0.0014	1.0×10^{-5}	3.3×10^{-6}

The maximum mass flow rate occurs during the worst case, quiet plasma conditions ($\lambda_d = 4$ m) as the net plasma current to the craft is at its highest level then. In a nominal plasma ($\lambda_d = 200$ m) mass flow rates are reduced by at least an order of magnitude. The mass flow rates are orders of magnitudes lower for positive charging as low mass electrons are emitted. The currents here are still higher, so a higher electrical power is required compared to the negative charging.

The highest expected mass flow rate for this combined MC system are below 8 μg/s for all expected plasma conditions. The current spacecraft charge control technology can produce mass flow rates as high as 0.1 A at 100 μg/s and 10 A at 200 μg/s.,[21,24] indicating this is an achievable target with current technology. Also, the mass flow rate analysis conducted here does not account

for any inefficiencies in the charge control device. In addition, the charge control accuracy for a TCS node system is not important, rather that the overall charge is significant to maintain tether tension and overcome external disturbances. For this reason, a higher mass flow rate will increase the nodal charge and ultimately add stiffness to the MC system.

Total Propellant Mass Comparison

For this MC TCS application example it is beneficial to estimate the total propellant mass required by the charge control system. The example used is the baseline MC system with spheres of 2 m and 0.5 m radii. The nodes are operating in an orbit normal configuration at GEO with a desired center to center separation of 7 m. With a Mother mass of 2000 kg and a Child mass of 50 kg the differential gravity force compressing the craft has a magnitude of 74.4 μN. In this naturally compressive orbit scenario, the repulsive Coulomb force maintains a taut tether and desired situational awareness separation. To achieve this force in a nominal plasma requires the nodes to be charged to $|12.2|$ kV. An advantage of the TCS concept here is that there is no need for sophisticated sensing and control. In addition there are no plume impingement concerns such as encountered if this scenario were implemented with free-flying craft with traditional chemical thrusters.

For the TCS system the total propellant mass is computed for both negative charging through emission of Xenon ions (Xe^+) and positive charging with electron (e^-) emission using the mass flow rates of Table 2. The charge emission is used to apply continuous thrust to oppose the differential gravity force, maintaining a 7 m separation for 10 years. The propellant mass flow rate is computed for a nominal plasma (λ_d = 200 m) in sunlit conditions.

The total propellant mass requirements are extremely low for a Coulomb system. If operating in a nominal GEO plasma environment, the TCS system requires 122.4 g of Xenon propellant for positive charging. For electrons the propellant requirement is only 0.0014 g. These propellant mass will increase considering inefficiencies of the system and variable plasma environments.

Another important consideration is the inert mass requirements of the charge control system. The charge control device inert mass is estimated to be low, in the low kg range, which matches well with current charge control technology as shown in the earlier charge control hardware section. As an example, charge control devices for current space missions have masses ranging from 19 kg on ATS-6[25] through to the more recent CLUSTER devices weighing only 1.85 kg each.[18,22] These are devices that could be feasibly implemented on the Mother and Child craft.

CHILD MASS EFFECTS

As previously mentioned charge control can be conducted on both the Mother and the Child or only on one craft that transfers charge via the interconnecting tether. The previous section outlined the range of mass required to charge a MC TCS. If charge control is conducted on the child craft, charging hardware and propellant requirements will impact the size and mass of the Child spacecraft. However, the mass of the Child craft will most likely be driven by what instruments it requires for its operations. Analyzed here is the effect of various Child masses on the relative dynamics of the baseline MC configuration. For launch purposes, minimal child mass is desirable, but at lower child masses the force induced from the charge control propellant emission may not be negligible. Because of this, a comparison of charge control emission force relative to the inflation Coulomb force is presented.

Relative Dynamics

The mass of the Child craft will depend on its function and its associated hardware requirements. Analyzed here is the effects of various masses on the relative dynamics of the MC TCS. Figure 10 shows the maximum relative rotations, maximum variation in separation distances and required control torques for various Child masses. The results in Figure 10 show that a lower mass Child reduces the relative dynamics and required control torque of the Mother. Figures 10(a) & 10(b) show that additional tethers provide increased stiffness of a MC TCS. However, similar to previous sections, multiple tethers have no effect on the required Mother attitude control.

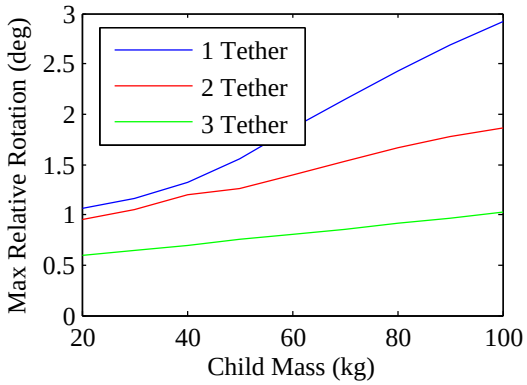

(a) Maximum Relative Rotation

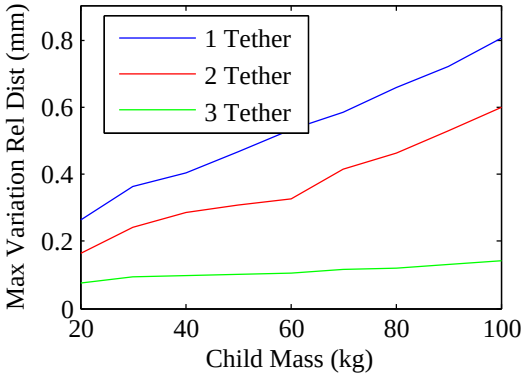

(b) Maximum Separation Distance Variation

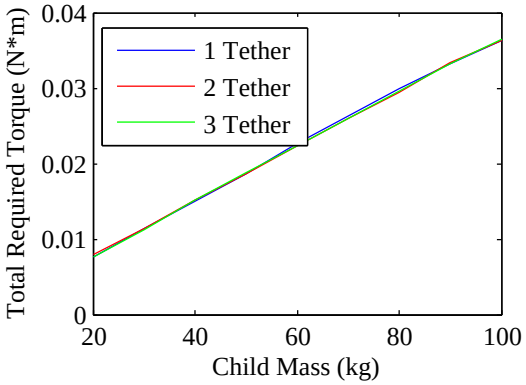

(c) Required Attitude Control Torque

Figure 10. Mother Child mass variation effects

Charge Emission Force and Node Accelerations

The charge current required to maintain a fixed potential is emitted under electrostatic acceleration. The emission current, while low magnitude, results in a net momentum exchange and consequently a force on the TCS nodes that feature charge control. In earlier studies this force is shown to be negligible for the free-flying charged spacecraft where Debye lengths are assumed to be at least 80 meters or larger.[3] However, these Debye length values are not sufficiently conservative, hence the use of the worst case plasma conditions of this study (λ_d = 4 m). In addition, if a charge control device is implemented on the low mass Child spacecraft it may experience relatively large

accelerations due to the charge emission force. The charge-thrust force is computed for each of the plasma conditions and compared to the magnitude of the Coulomb force produced for the baseline MC system. The force on a node from the emission current is computed using:[26]

$$F_{cc} = \dot{m} u_{ion} \tag{17}$$

where u_{ion} is the emission speed of the ions. During positive charging, low mass electrons are emitted. The mass flow rate is computed using Eq. (16) and the emitted ion species is assumed to be Xenon here. The emission speed is proportional to the spacecraft potential V_{sc} and is calculated using electrostatic repulsion:[26]

$$u_{ion} = \sqrt{\frac{2 e_c V_{sc}}{m_{ion}}} \tag{18}$$

Combining Equations (16), 17 & 18 the net charge control force is computed with:

$$F_{cc} = I_{\text{net}} \sqrt{\frac{2 m_{ion} V_{sc}}{e_c}} \tag{19}$$

The magnitude of the charge emission force is compared as a ratio of the Coulomb force and shown in Figure 11. This total emission force is computed for both the Mother and Child combined in each of the three representative plasmas. The lower shaded region indicates where the charge emission force is greater than the Coulomb force at that potential.

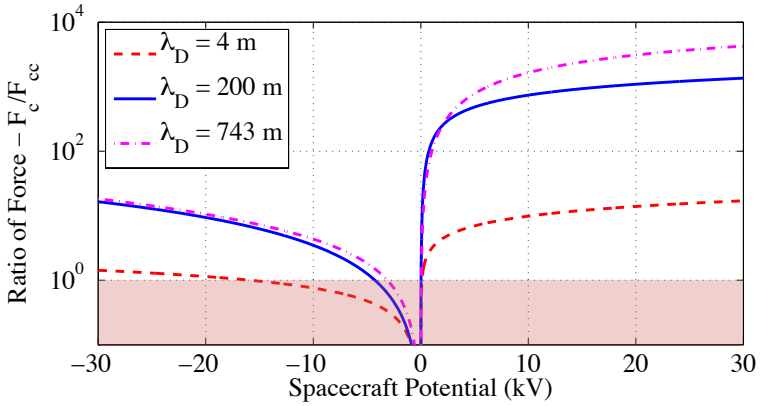

Figure 11 Ratio of Coulomb force : Charge emission force for the Mother Child system in different plasmas.

It is desirable to have a large ratio between these forces given that the Coulomb force is our inflationary actuator and the charge emission force is seen as a potential disturbance on the system. For positive charging the emission of low mass electrons gives a suitably large ratio (> 10 for the worst case plasma). However due to the higher momentum transfer of the Xenon ions during negative charging the ratio between the forces is reduced. In the worst case plasma the forces are very similar magnitude. In the nominal and disturbed plasmas the charge emission force is approximately an order of magnitude less than the minimum Coulomb inflation force.

This study indicates that consideration for the placement and direction of the charge control device on the nodes should be made. If a single charge control device on the Mother is used to charge

the system, the emission force can be close or even greater than the Coulomb force magnitudes during negative charging and worst-case plasma conditions. With appropriate placement and the use of multiple emitters the emission force can be directed to create zero net force on the node and not interfere with Coulomb inflation forces. A conceptual example of a charged node with zero net force charge emission plumes is shown in Figure 12. In addition, correct placement of the charge device on the Mother or Child could be used as an additional torque source to assist in controlling external perturbations such as gravity gradients.

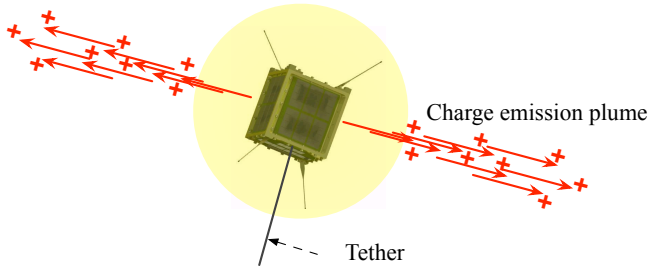

Figure 12. Illustration of bi-directional charge emission on a tethered spacecraft node

CONCLUSION

This paper analyzes the use of a Tethered Coulomb Structure for situational awareness of a GEO satellite by tethering a small Child craft to a large Mother craft. This study demonstrates that the Mother Child TCS application for situational awareness provides a close proximity fixed sensor platform and is feasible for achievable charge and propellant mass requirements. By implementing a simple attitude control law on the Mother craft, the MC formation can hold its orientation fixed relative to the orbit frame with little relative translation and rotation between the Mother and the Child. Using multiple tethers between the craft allows for separation distance of upwards of 10 m with relative rotations less than 5 degrees.

Examination of power required to maintain fixed potentials shows that under nominal space weather conditions only Watt levels of power are required. Variation of the spacecraft radius and polarity shows that larger radii craft and positive polarity charging requires more power. Additionally, simulations show that MC system stiffness increases rapidly with increasing potential until it plateaus around 30 kV.

Propellant mass requirements for the MC concept is directly related to the polarity of spacecraft charging. Negative charging requires several orders of magnitude larger propellant mass than positive charging because of the mass variation between electrons and ions. However, charging to negative potentials only requires 122.4 g of propellant for a ten year mission, which is very comparable to other electric propulsion methods.

Lastly, this study examines various Child masses and shows that lower Child masses improves the stiffness of a MC by reducing relative translations, rotation, and required torque. However, lower Child masses could result in non-negligible accelerations being imposed on the Child by the charging device. Even so, these acceleration could be harnessed and used to provide more system rigidity with intelligent spacecraft design.

REFERENCES

[1] O. Mori, Y. Shirasawa, Y. Miyazaki, H. Sakamoto, M. Hasome, N. Okuizumi, H. Sawada, H. Furuya, S. Matunga, M. Natori, and J. Kawaguchi, "Deployment and Steering Dynamics of Spinning Solar Sail "IKAROS"," tech. rep., Japan Aerospace Exploration Agency, 2010.

[2] H. Schaub and J. L. Junkins, *Analytical Mechanics of Space Systems*. Reston, VA: AIAA Education Series, 2nd ed., October 2009.

[3] L. B. King, G. G. Parker, S. Deshmukh, and J.-H. Chong, "Spacecraft Formation-Flying using Inter-Vehicle Coulomb Forces," tech. rep., NASA Institute for Advanced Concepts (NIAC), January 2002.

[4] H. Schaub, G. G. Parker, and L. B. King, "Challenges and Prospect of Coulomb Formations," *Journal of the Astronautical Sciences*, Vol. 52, Jan.–June 2004, pp. 169–193.

[5] D. W. Miller, , R. J. Sedwick, E. M. C. Kong, and S. Schweighart, "Electromagnetic Formation Flight for Sparse Aperture Telescopes," *IEEE Aerospace Conference Proceedings – Volume 2*, Big Sky, Montana, March 9–16 2002.

[6] J. Gersh, "Architecting the Very-Large-Aperture Flux-Pinned Space Telescope: A Scalable, Modular Obtical Array with High Agility and Passively Stable Orbital Dynamics," *AAS/AIAA Astrodynamics Specialist Conference*, Honolulu, Hawaii, Aug. 18–21 2008.

[7] M. A. Peck, B. Streetman, C. M. Saaj, and V. Lappas, "Spacecraft Formation Flying using Lorentz Forces," *Journal of British Interplanetary Society*, Vol. 60, July 2007, pp. 263–267.

[8] H. Schaub, G. G. Parker, and L. B. King, "Coulomb Thrusting Application Study," tech. rep., Virginia Tech and Aerophysics, Jan. 2006.

[9] C. R. Seubert and H. Schaub, "Tethered Coulomb Structures: Prospects and Challenges," *AAS F. Landis Markley Astrodynamics Symposium*, Cambridge, MA, June 30 – July 2 2008. Paper No. AAS 08–269.

[10] C. R. Seubert and H. Schaub, "Impact of Nodal Attitude Motion on Two-Element Tethered Coulomb Structures," *AAS/AIAA Spaceflight Mechanics Meeting*, San Diego, CA, Feb. 14-17 2010. Paper No. AAS 10–268.

[11] C. R. Seubert, S. Panosian, and H. Schaub, "Dynamic Feasibility Study of a Tethered Coulomb Structure," *AAS/AIAA Astrodynamics Specialist Conference*, Toronto, Canada, Aug. 2–5 2010. Paper No. AIAA-2010–8131.

[12] D. A. Gurnett and B. A., *Introduction to Plasma Physics - with Space and Laboratory Applications*. New York, NY: Cambridge University Press, 2005. Pages 8–9.

[13] E. C. Whipple, "Potentials of surfaces in space," *Reports on Progress in Physics*, Vol. 44, No. 11, 1981, pp. 1197–1250.

[14] N. Murdoch, D. Izzo, C. Bombardelli, I. Carnelli, A. Hilgers, and D. Rodgers, "Electrostatic Tractor for Near Earth Object Deflection," *59th International Astronautical Congress*, Glasgow, Scotland, 2008. Paper IAC-08-A3.I.5.

[15] J. Sliško and R. Brito-Orta, "On Approximate Formulas for the Electrostatic Force Between Two Conducting Spheres," *American Journal of Physics*, Vol. 66, April 1998, pp. 352–355.

[16] W. R. Smythe, *Static and Dynamic Electricity*. McGraw-Hill, 3rd ed., 1968.

[17] S. T. Lai and M. Tautz, "High-Level Spacecraft Charging at Geosynchronous Altitudes: A Statistical Study," *8th Spacecraft Charging Technology Conference*, Oct. 2003.

[18] W. Riedler, K. Torkar, F. Rudenauer, M. Fehringer, A. Pedersen, R. Schmidt, R. J. L. Grard, H. Arends, B. T. Narheim, J. Troim, R. Torbert, R. C. Olsen, E. Whipple, R. Goldstein, N. Valavanoglou, and H. Zhao, "Active Spacecraft Potential Control," *Space Science Reviews*, Vol. 79, Jan. 1997, pp. 271–302.

[19] W. D. Deininger, G. Aston, and L. C. Pless, "Hollow-cathode plasma source for active spacecraft charge control," *Review of Scientific Instruments*, Vol. 58, June 1987, pp. 1053–1062. -19 kV potential ATS 6.

[20] S. T. Lai, "An overview of electron and ion beam effects in charging and discharging of spacecraft," *IEEE Transactions on Nuclear Science*, Vol. 36, Dec. 1989, pp. 2027–2032.

[21] G. Aston, A. M. B., and J. D. Williams, "Miniature Plasma Activated Systems for Tether Current Generation," *Space Technology and Applications International Forum* (A. I. o. Physics, ed.), 2001.

[22] K. Torkar, W. Riedler, C. P. Escoubet, M. Fehringer, R. Schmidt, G. R. J. L., H. Arends, F. Rudenauer, W. Steiger, B. T. Narheim, K. Svenes, R. Torbert, A. M., A. Fazakerley, R. Goldstein, R. C. Olsen, A. Pedersen, E. Whipple, and H. Zhao, "Active Spacecraft Potential Control for Cluster – Implementation and First Results," *Annales Geophysicae*, Vol. 19, No. 10/12, 2001, pp. 1289–1302.

[23] K. Torkar, M. Fehringer, H. Arends, R. Goldstein, R. J. L. Grard, B. T. Narheim, R. C. Olsen, A. Pedersen, W. Riedler, F. Rudenauer, R. Schmidt, K. Svenes, E. Whipple, R. Torbert, and H. Zhao, "Spacecraft Potential Control using Indium Ion Source – Experience and Outlook Based on Six Years of Operation in Space," *6th Spacecraft Charging Control Technology Conference*, Hanscom AFB, MA, Sept. 2000. AFRL-VS-TR-20001578.

[24] C. M. Marrese, "A Review of Field Emission Cathode Technologies for Electric Propulsion Systems and Instruments," *IEEE Aerospace Conference Proceedings*, Vol. 4, 2000, pp. 85–98.

[25] B. M. Shuman, H. A. Cohn, J. Hyman, R. R. Robson, J. Santoru, and W. S. Willamson, "Automatic Charge Control System for Geosynchronous Satellites," *Journal of Electrostatics*, Vol. 20, 1987, pp. 141–154.

[26] D. M. Goebel and I. Katz, *Fundamentals of Electric Propulsion*. JPL Space Science and Technology Series, Hoboken, NJ: John Wiley and Sons, 2008.